BIOCHEMISTRY
including biophysical chemistry & molecular biology

Article

pubs.acs.org/biochemistry

Effects of Ammonia on the Structure of the Oxygen-Evolving Complex in Photosystem II As Revealed by Light-Induced FTIR Difference Spectroscopy

Li-Hsiu Hou, Chia-Ming Wu, Hsin-Ho Huang, and Hsiu-An Chu*

Institute of Plant and Microbial Biology, Academia Sinica, Taipei 11529, Taiwan

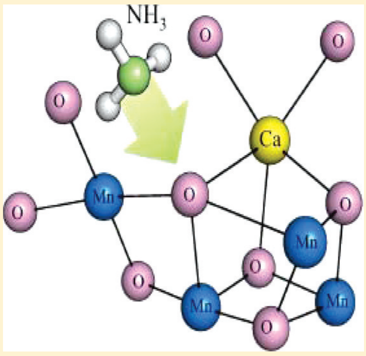

ABSTRACT: NH_3 is a structural analogue of substrate H_2O and an inhibitor to the water oxidation reaction in photosystem II. To test whether or not NH_3 is able to replace substrate water molecules on the oxygen-evolving complex in photosystem II, we studied the effects of NH_3 on the high-frequency region (3750−3550 cm^{-1}) of the $S_2Q_A^-/S_1Q_A$ FTIR difference spectra (pH 7.5 at 250 K), where OH stretch modes of weak hydrogen-bonded active water molecules occur. Our results showed that NH_3 did not replace the active water molecule on the oxygen-evolving complex that gave rise to the S_1 mode at ∼3586 cm^{-1} and the S_2 mode at ∼3613 cm^{-1} in the $S_2Q_A^-/S_1Q_A$ FTIR difference spectrum of PSII. In addition, our mid-frequency FTIR results showed a clear difference between pH 6.5 and 7.5 on the concentration dependence of the NH_4Cl-induced upshift of the S_2 state carboxylate mode at 1365 cm^{-1} in the $S_2Q_A^-/S_1Q_A$ spectra of NH_4Cl-treated PSII samples. Our results provided strong evidence that NH_3 induced this upshift in the spectra of NH_4Cl-treated PSII samples at 250 K. Moreover, our low-frequency FTIR results showed that the Mn−O−Mn cluster vibrational mode at 606 cm^{-1} in the $S_2Q_A^-/S_1Q_A$ spectrum of the NaCl control PSII sample was diminished in those samples treated with NH_4Cl. Our results suggest that NH_3 induced a significant alteration on the core structure of the Mn_4CaO_5 cluster in PSII. The implication of our findings on the structure of the NH_3-binding site on the OEC in PSII will be discussed.

Photosystem II (PSII) is a multisubunit membrane protein complex in the thylakoid membrane that functions as a water−plastoquinone oxidoreductase.[1,2] It couples light-induced charge separation with the oxidation of water to molecular oxygen and the reduction of the plastoquinone acceptors Q_A and Q_B. The water oxidation chemistry occurs in an oxygen-evolving complex (OEC), consisting of a Mn_4CaO_5 cluster.[1] NH_3 is a structural analogue of substrate H_2O and an inhibitor to the water oxidation reaction in Photosystem II (PSII).[3−6] EPR studies on NH_3-treated PSII samples at alkaline pHs near 7.5 demonstrated that alterations of the S_2 state multiline EPR signal occur when samples that have been illuminated at 200 K are subsequently "annealed" above 250 K or when samples that are poised in the dark-stable S_1 state are illuminated above 250 K.[7,8] These results appeared to show that NH_3 binds directly to the Mn site after the S_2 state forms.[7,8] An ESEEM study performed on the NH_3-altered multiline EPR signals at pH 7.5 concluded that a single NH_3-derived ligand binds directly to the Mn cluster in the S_2 state.[9] In addition, this ESEEM study provided evidence that ammonia may form an amido (NH_2) bridge between metal ions.[9] An extended X-ray absorption fine structure (EXAFS) study on NH_3-treated PSII samples at pH 7.5 reported an elongation of one binuclear center in the Mn cluster which could result from the replacement of one bridging μ-oxo by an amido group.[10]

We previously applied FTIR difference spectroscopy to study the effect of NH_3 on OEC structural changes during S_1 to S_2 state transition at 250 K.[11,12] Our results showed that NH_4Cl induced several characteristic spectral changes in the amide and carboxylate stretch regions of the $S_2Q_A^-/S_1Q_A$ spectra.[11,12] Among them, the S_2 state carboxylate mode at 1365 cm^{-1} in the $S_2Q_A^-/S_1Q_A$ spectrum of the controlled samples upshifted to 1379 cm^{-1} in NH_3-treated samples without significant overlap with other protein modes. Therefore, we used the upshift of this carboxylate mode to measure the effect of NH_3.[11,12] This carboxylate mode has been assigned to a Mn-ligating carboxylate whose coordination mode changes from bridging or chelating to unidentate ligation during the S_1 to S_2 transition.[13] On the basis of the correlations between the conditions that gave rise to the NH_3-induced upshift of the 1365 cm^{-1} mode and the conditions that gave rise to the modified S_2 state multiline EPR signal, our previous FTIR results suggested that the NH_3-induced upshift of the 1365 cm^{-1} mode was caused by the binding of NH_3 to the Mn site on the PSII/OEC which give rise to the altered S_2 state multiline EPR signal.[11] We also found that ethylene glycol alters the steric requirement of the amine effect on the upshift of the 1365 cm^{-1} mode in the $S_2Q_A^-/S_1Q_A$ spectrum at 250 K.[12] In PSII samples containing 30% (v/v) ethylene glycol, only NH_3, not other bulkier amines (e.g., Tris, AEPD and CH_3NH_2), has a clear effect on the mentioned upshift; this contrasts with PSII samples containing 0.4 M sucrose, on which both NH_3 and CH_3NH_2 have a clear effect.[12]

Received: June 20, 2011
Revised: September 26, 2011
Published: September 27, 2011

On the basis of the above results, we proposed that ethylene glycol, whether acting directly or indirectly, decreases the affinity or limits the accessibility of NH_3 and CH_3NH_2 to the NH_3-specific binding site on the OEC in PSII at 250 K.[12]

A recent FTIR study reported that the ammonium cations have an inhibitory effect on the PSII/OEC.[14] The NH_4Cl treatment at pH 6.5 and 5.5 induced significant changes in the COO^- stretching regions in flash-induced S_2/S_1 FTIR difference spectra of PsbP- and PsbQ-depleted PSII membranes at 283 K. The NH_4Cl concentration dependence on the amplitude of the spectral changes showed a positive correlation with the inhibition of oxygen evolution.[14] This study proposed that the ammonium cations may interact with carboxylate groups coupled to the Mn cluster (as direct ligands or proton transfer mediators) and inhibit the oxygen evolution reaction.[14] In addition, the COO^- changes are totally different from the band shift at 250 K, thus indicating different carboxylate group perturbations.[14]

The vibrational modes of water molecules on the PSII/OEC were studied by Noguchi and colleagues using FTIR difference spectroscopy.[15−18] A pair of positive and negative bands was observed at 3618 and 3585 cm^{-1}, respectively, in a flash-induced S_2/S_1 FTIR difference spectrum of PSII core complexes from *Thermosynechococcus elongates* at pH 6.5.[16] Both of these bands exhibited 12 cm^{-1} downshifts when the $H_2{}^{16}O$ buffer was replaced by $H_2{}^{18}O$.[16] Upon D_2O substitution, the bands largely shifted down to 2681 and 2652 cm^{-1}. These observations indicate that the bands at 3618 and 3585 cm^{-1} arise from the OH stretching vibrations of a water molecule, probably substrate water, coupled to the Mn cluster in the S_2 and S_1 states, respectively.[16] The band frequencies indicate that the OH group forms a weak H-bond that further weakens upon S_2 formation. Noguchi and colleagues also reported the flash-induced difference spectra of S-state transitions in the weakly H-bonded OH stretching region.[18] The water (or hydroxide) molecules detected in the FTIR difference spectra are potential candidates for substrate water molecules in PSII water oxidation reactions.[15]

In this work, we report effects of NH_4Cl on the high-frequency region where OH stretching modes of active water molecules occur and on the low-frequency region of $S_2Q_A^-/S_1Q_A$ FTIR difference spectra at 250 K where the Mn−O−Mn cluster vibration mode of the OEC occurs. We will discuss the implication of our findings on the structure of the ammonia-binding site on the OEC in PSII.

■ MATERIALS AND METHODS

Sample Conditions for FTIR Measurement. Spinach OTG PSII reaction center cores (RCCs), retaining the three extrinsic polypeptides, were prepared as described in ref 19. Typical oxygen evolution rates were about 1.1−1.4 mmol of O_2 (mg of Chl)$^{-1}$ h^{-1}. NH_4Cl-treated PSII samples were prepared from PSII OTG RCCs. For high-frequency FTIR experiments, the RCCs were washed twice with HEPES buffer (40 mM HEPES, 10 mM NaCl, and 5 mM $CaCl_2$, at pH 7.5). NH_4Cl was added from a 1.25 M stock solution (pH was adjusted to pH 7.5) to a final concentration of 50 mM. For the $S_2Q_A^-/S_1Q_A$ FTIR difference spectra, the sample suspension included 0.1 mM DCMU. For the Q_A^-/Q_A FTIR difference spectra, the sample suspension included 0.1 mM DCMU and 10 mM NH_2OH. The sample suspension was placed on one AgCl sample window and gently dried under a stream of N_2 gas for 5 min. The sample suspension was spread more evenly on the AgCl window than on the CaF_2 window. The partially dehydrated sample (on the sample window) was incubated with 20% glycerol for 10 min in a small sealed compartment in a home-built humidifier. After incubation, the newly humidified sample was quickly sandwiched with a new CaF_2 window for FTIR experiments.

For pH-dependent mid-frequency FTIR experiments, the RCCs were washed with HEPES buffer (40 mM HEPES, 10 mM NaCl, 5 mM $CaCl_2$, and 0.4 M sucrose, at pH 7.5) or Mes buffer (50 mM Mes, 10 mM NaCl, 5 mM $CaCl_2$, and 0.4 M sucrose, at pH 6.5). Samples were then centrifuged 30 min at 13 000 rpm to produce a pellet. The pellet was then sandwiched between two CaF_2 sample windows. $^{15}NH_4Cl$ with 98+ atom % ^{15}N was purchased from Aldrich Chemical Co. For low-frequency FTIR experiments, spinach HTG RCCs were prepared as described.[20] Typical oxygen evolution rates were about 1.3−1.8 mmol of O_2 (mg of Chl)$^{-1}$ h^{-1}. HTG PSII RCCs were used for low-frequency FTIR experiments because they had significantly higher activity than did OTG PSII RCCs, which slightly improved the signal-to-noise ratio of our low-frequency FTIR spectra. Samples were centrifuged 30 min at 13 000 rpm to produce a pellet. The pellet was then sandwiched between two AgCl or AgBr sample windows for FTIR experiments.

Experimental Conditions for FTIR Measurement. Mid-frequency FTIR experiments were performed on a Burker Vortex 77 spectrometer that was equipped with a KBr beam splitter and a MCT detector. Low-frequency FTIR experiments were performed on a Burker Vortex 77 spectrometer that was equipped with a KBr beam splitter and a liquid-He cooled Si Bolometer. Samples were cooled to 250 K using an Oxford DN liquid nitrogen cryostat and their temperature was regulated to ±0.1 K using a temperature controller (Oxford ITC 502). Samples were illuminated for four seconds using a Dolan-Jenner MI 150 high-intensity illuminator with infrared and red cutoff filters. The acquisition time for all spectra was 1 min (387 scans). The light-minus-dark difference spectrum was obtained from the ratio of the single-beam dark spectrum and the one following illumination. The spectral resolution for all spectra was 4 cm^{-1}.

■ RESULTS

Figure 1 shows the weakly H-bonded OH stretching region of the $S_2Q_A^-/S_1Q_A$ FTIR difference spectra of partially dehydrated OTG PSII RCC samples with 50 mM NaCl (thick blue line), 50 mM $^{14}NH_4Cl$ (thick red line), or 50 mM $^{15}NH_4Cl$ (thick green line). Spinach OTG PSII RCCs retained the three critical extrinsic polypeptides for maintaining the activity of samples under partially dehydrated experimental conditions. The positive band at ∼3612 cm^{-1} and the negative band at ∼3584 cm^{-1} in the $S_2Q_A^-/S_1Q_A$ spectrum of spinach PSII samples (Figure 1) corresponds to bands at ∼3618 and ∼3585 cm^{-1} in the S_2/S_1 difference spectrum of *Thermosynechococcus elongatus* PSII core complexes.[16] These modes were previously assigned to the weakly H-bonded OH stretch modes of one active water molecule undergoing structural changes during the S_1 to S_2 transition of the PSII/OEC.[16] Our results conclude that NH_3 did not replace this active water molecule on the OEC. In addition, we observed that NH_4Cl-induced small frequency shifts (about 3 cm^{-1}) of these two modes in the $S_2Q_A^-/S_1Q_A$ spectra of NH_3-treated PSII samples. These spectral changes can be resolved into a positive feature at 3605 cm^{-1} and a negative feature at 3590 cm^{-1} in the double difference NH_4Cl-minus-NaCl and $S_2Q_A^-/S_1Q_A$ FTIR spectrum of PSII (thick black line). In contrast, there is no significant spectral change in double difference $^{15}NH_4Cl$-minus-$^{14}NH_4Cl$ and $S_2Q_A^-/S_1Q_A$

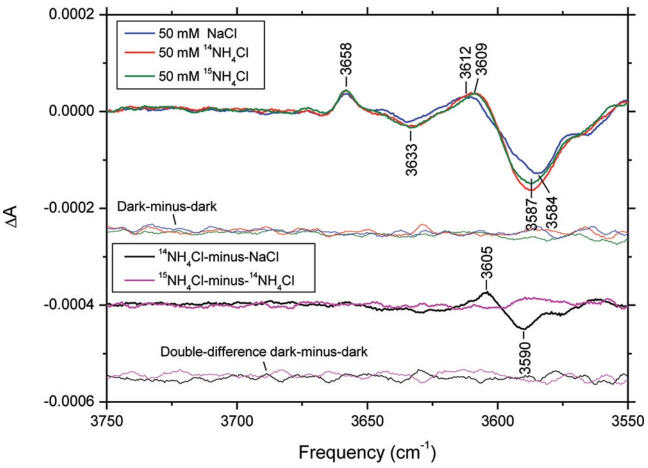

Figure 1. Weakly H-bonded OH-stretch modes of the active water in $S_2Q_A^-/S_1Q_A$ FTIR difference spectra of PSII samples with 50 mM NaCl (thick blue line), 50 mM $^{14}NH_4Cl$ (thick red line), or 50 mM $^{15}NH_4Cl$ (thick green line). The sample suspension included 0.1 mM DCMU. The FTIR measurement was performed at 250 K. Spectra obtained with 8−11 samples were averaged. The dark-minus-dark spectra (thin line) were recorded immediately before the light-minus-dark-spectra. It gives an indication of the noise level in light-minus-dark FTIR difference spectra. The double-difference $^{14}NH_4Cl$-minus-NaCl spectrum (thick black line) shown at the bottom was obtained by subtracting the $S_2Q_A^-/S_1Q_A$ FTIR difference spectrum of PSII samples with 50 mM NaCl (thick blue line) from the $S_2Q_A^-/S_1Q_A$ FTIR difference spectrum of PSII samples with 50 mM $^{14}NH_4Cl$ (thick red line). The double-difference $^{15}NH_4Cl$-minus-$^{14}NH_4Cl$ spectrum (thick magenta line) shown at the bottom was obtained by subtracting the $S_2Q_A^-/S_1Q_A$ FTIR difference spectrum of PSII samples with 50 mM $^{14}NH_4Cl$ (thick red line) from the $S_2Q_A^-/S_1Q_A$ FTIR difference spectrum of PSII samples with 50 mM $^{15}NH_4Cl$ (thick green line).

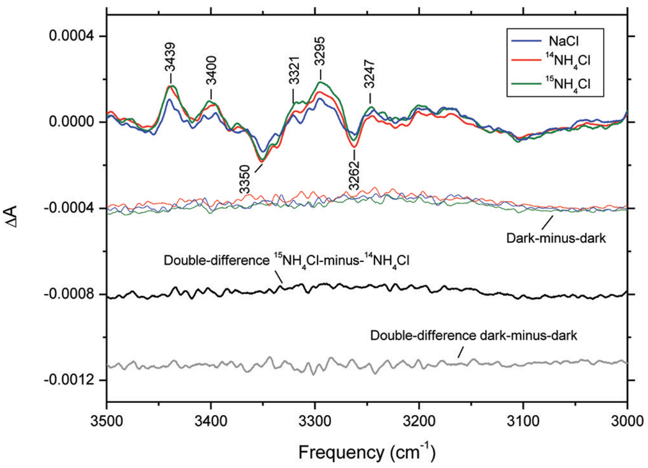

Figure 2. The NH stretching region in $S_2Q_A^-/S_1Q_A$ FTIR difference spectra of PSII samples with 50 mM NaCl (thick blue line), 50 mM $^{14}NH_4Cl$ (thick red line), or 50 mM $^{15}NH_4Cl$ (thick green line). Experimental conditions are the same as in Figure 1. The double difference $^{15}NH_4Cl$-minus-$^{14}NH_4Cl$ spectrum (thick black line) shown at the bottom was obtained by subtracting the $S_2Q_A^-/S_1Q_A$ FTIR difference spectrum of PSII samples with 50 mM $^{14}NH_4Cl$ (thick red line) from that of PSII samples with 50 mM $^{15}NH_4Cl$ (thick green line). The double-difference dark-minus-dark spectrum (thick gray line) shown at the bottom was obtained by subtracting the dark-minus-dark spectrum of $^{14}NH_4Cl$-treated PSII samples (thin red line) from the dark-minus-dark spectrum of $^{15}NH_4Cl$-treated PSII samples (thin green line). It gives an indication of the noise level in the double-difference $^{15}NH_4Cl$-minus-$^{14}NH_4Cl$ spectrum (thick black line).

FTIR spectra of PSII (thick magenta line). Therefore, these spectral changes were not derived from the vibrational mode involved in NH_3 but from a slight change in the OH stretch modes of the active water induced by NH_4Cl.

Figure 2 shows the NH stretching region of $S_2Q_A^-/S_1Q_A$ FTIR difference spectra of partially dehydrated PSII samples with 50 mM NaCl (thick blue line), 50 mM $^{14}NH_4Cl$ (thick red line), or 50 mM $^{15}NH_4Cl$ (thick green line). The NH stretching vibrations of ammine (NH_3), amido (NH_2) complexes and H-bonded NH_3 molecules are expected to be present at 3400−3000 cm^{-1}.[21] The asymmetric and symmetric NH stretching vibrational modes of metal-bound NH_3 generally show a ^{15}N-induced shift of 5−10 cm^{-1}.[21] As shown in Figure 2, we found no significant differences in the NH stretching vibration region (3400−3000 cm^{-1}) of the double-difference $^{15}NH_4Cl$-minus-$^{14}NH_4Cl$ $S_2Q_A^-/S_1Q_A$ FTIR spectrum of PSII. We hypothesize that the NH stretching modes of the manganese-bound NH_3 might be too broad to be detected in our spectra. In fact, the strongly H-bonded of OH stretching vibrational modes of H_2O are expected to appear around 3400 cm^{-1} were not identified in the S_2/S_1 FTIR difference spectrum presumably due to their very weak extinction coefficient. In addition, the OH and NH stretching modes of the protein backbones and side chains are expected to appear in the 3450−3250 cm^{-1} region.[22] Several bands were observed in the 3500−3000 cm^{-1} region of spectra in Figure 2, which are not sensitive to the $^{15}NH_4Cl$ isotope exchange. These bands might originate from the OH and NH stretching modes of the protein backbones and side chains.[22]

Figure 3 shows the mid-frequency region of $S_2Q_A^-/S_1Q_A$ FTIR difference spectra of partially dehydrated PSII samples with 50 mM NaCl (blue line), 50 mM $^{14}NH_4Cl$ (red line), or 50 mM $^{15}NH_4Cl$ (green line). Our results showed that NH_4Cl induced several characteristic spectral changes in the region of symmetric carboxylate stretching modes (1450−1300 cm^{-1}) of the $S_2Q_A^-/S_1Q_A$ spectrum of PSII.[11] Among them, the S_2 state carboxylate mode at 1365 cm^{-1} in the $S_2Q_A^-/S_1Q_A$ spectrum of

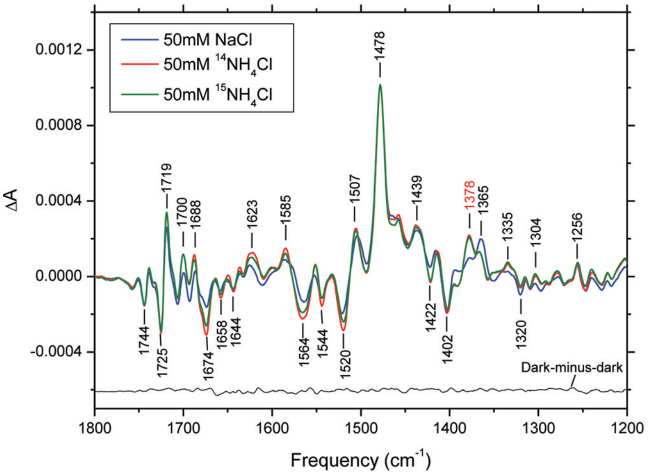

Figure 3. Mid-frequency $S_2Q_A^-/S_1Q_A$ FTIR difference spectra of PSII samples with 50 mM NaCl (blue line), 50 mM $^{14}NH_4Cl$ (red line), or 50 mM $^{15}NH_4Cl$ (green line). Experimental conditions are the same as in Figure 1.

control PSII samples was clearly upshifted to ∼1378 cm^{-1} in NH_4Cl-treated samples. Because this carboxylate mode showed a clear frequency upshift without overlapping with other protein bands in the $S_2Q_A^-/S_1Q_A$ spectra, this upshift was used to measure NH_4Cl effects.

Figure 4 shows the weakly H-bonded OH-stretching region of Q_A^-/Q_A FTIR difference spectra of partially dehydrated PSII samples with 50 mM NaCl (thick blue line) or 50 mM NH_4Cl (thick red line). The positive bands at 3658 and 3602 cm^{-1} and a negative band at 3580 cm^{-1} are present in both Q_A^-/Q_A spectra of the controlled and NH_3-treated samples. The positive band at 3658 cm^{-1} is sensitive to D_2O and ^{18}O water exchanges (data not shown) and can be tentatively assigned to the OH stretching mode of a weakly H-bonded water molecule, which is structurally coupled to the reduction of the Q_A acceptor. In addition, there is no significant spectral change in the double difference NH_4Cl-minus-NaCl and Q_A^-/Q_A FTIR spectrum of PSII (thick black line). Therefore, these above vibrational modes in the Q_A^-/Q_A spectra are not sensitive to the NH_4Cl treatment.

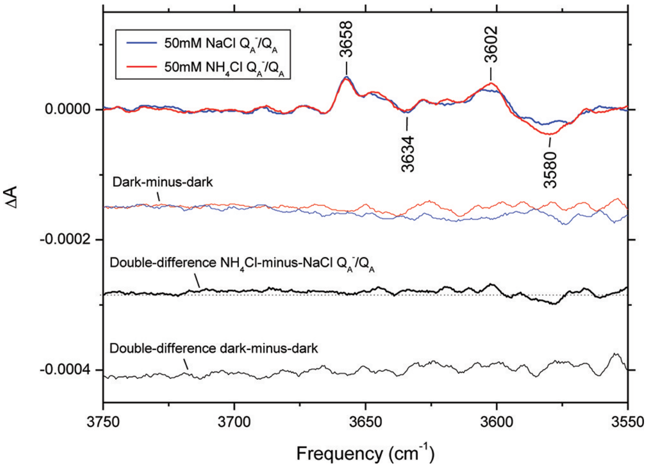

Figure 4. Weakly H-bonded OH stretch modes of the active water in Q_A^-/Q_A FTIR difference spectra of PSII samples with 50 mM NaCl (thick blue line) or 50 mM NH_4Cl (thick red line). The sample suspension included 0.1 mM DCMU and 10 mM NH_2OH. The FTIR measurement was performed at 250 K. Spectra obtained with 9−11 samples were averaged. Dark-minus-dark spectra of PSII samples with 50 mM NaCl (thin blue line) or 50 mM NH_4Cl (thin red line) give an indication of the noise level in the Q_A^-/Q_A FTIR difference spectra. The double difference NH_4Cl-minus-NaCl Q_A^-/Q_A spectrum (thick black line) was obtained by subtracting the Q_A^-/Q_A FTIR difference spectrum of PSII samples with 50 mM NaCl (thick blue line) from that of PSII samples with 50 mM NH_4Cl (thick red line). The double-difference dark-minus-dark spectrum (thin black line) shown at the bottom was obtained by subtracting the dark-minus-dark spectrum of NaCl-treated PSII samples (thin blue line) from the dark-minus-dark spectrum of NH_4Cl-treated PSII samples (thin red line). It gives an indication of the noise level in the double-difference NH_4Cl-minus-NaCl Q_A^-/Q_A spectrum (thick black line).

Figure 5 shows double-difference S_2/S_1 spectra of partially dehydrated PSII samples with 50 mM NaCl (thick blue line) or 50 mM NH_4Cl (thick red line). Each S_2/S_1 spectrum was obtained by subtracting the light-induced Q_A^-/Q_A difference spectrum (in Figure 4) from the light-minus-dark $S_2Q_A^-/S_1Q_A$ FTIR difference spectrum (in Figure 1). The intensity of each spectrum has been normalized with respect to the Q_A^- band at 1478 cm^{-1}. The S_2 mode at ∼3613 cm^{-1} and the S_1 mode at ∼3586 cm^{-1} are present in the double difference S_2/S_1 spectrum of control samples (thick blue line). The S_2 mode at ∼3611 cm^{-1} and the S_1 mode at ∼3588 cm^{-1} are present in the double difference S_2/S_1 spectrum of NH_3-treated samples (thick red line). In addition, the NH_3-induced spectral change can be resolved into a positive feature at 3605 cm^{-1} and a negative feature at 3590 cm^{-1} in the double-difference NH_4Cl-minus-NaCl S_2/S_1 spectrum of PSII (thick black line).

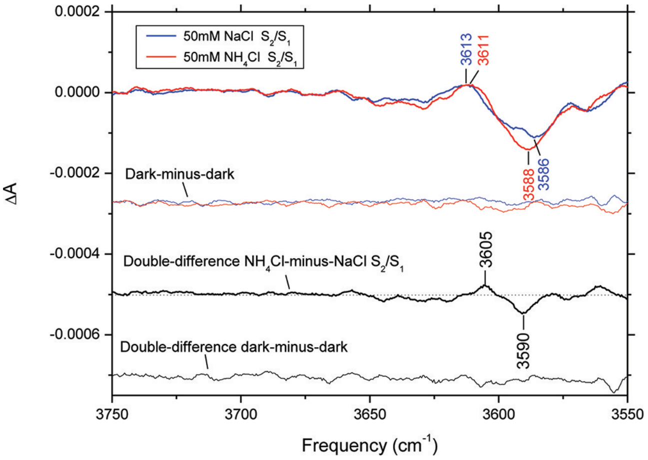

Figure 5. Weakly H-bonded OH stretch modes of the active water in double-difference S_2/S_1 FTIR difference spectra of PSII samples with 50 mM NaCl (thick blue line) or 50 mM NH_4Cl (thick red line). Each S_2/S_1 spectrum was obtained by subtracting the light-induced Q_A^-/Q_A difference spectrum (in Figure 4) from the light-minus-dark $S_2Q_A^-/S_1Q_A$ FTIR difference spectrum (in Figure 1). Each dark-minus−dark spectrum (thin line) was obtained by subtracting the dark-minus-dark spectrum of NH_2OH-treated PSII samples (in Figure 4) from dark-minus-dark spectrum of PSII samples (in Figure 1). It gives an indication of the noise level in the double-difference S_2/S_1 FTIR difference spectra of PSII. The double-difference NH_4Cl-minus-NaCl S_2/S_1 spectrum (thick black line) shown at the bottom was obtained by subtracting the S_2/S_1 spectrum of NaCl-treated PSII samples (thick blue line) from the S_2/S_1 spectrum of NH_4Cl-treated PSII samples (thick red line). The double-difference dark-minus-dark spectrum (thin black line) shown at the bottom was obtained by subtracting the dark-minus-dark spectrum of NaCl-treated PSII samples (thin blue line) from dark-minus-dark spectrum of NH_4Cl-treated PSII samples (thin red line). It gives an indication of the noise level in the double difference NH_4Cl-minus-NaCl S_2/S_1 FTIR difference spectrum of PSII (thick black line).

Figure 6 shows mid-frequency $S_2Q_A^-/S_1Q_A$ FTIR difference spectra of hydrated PSII samples with 10 mM NH_4Cl at pH 6.5 (green line), 100 mM NH_4Cl at pH 6.5 (blue line), 10 mM NH_4Cl at pH 7.5 (magenta line), and 100 mM NH_4Cl at pH 7.5 (red line). We used the S_2 state carboxylate mode upshift at ∼1365 cm^{-1} to measure NH_4Cl effects. Both 10 mM NH_4Cl at pH 7.5 (magenta line) and 100 mM NH_4Cl at pH 6.5 (blue line) conditions were able to induce the same upshift of the S_2 state carboxylate mode at ∼1365 cm^{-1} in the $S_2Q_A^-/S_1Q_A$ spectra of NH_3-treated samples as the condition with 100 mM NH_4Cl at pH 7.5 (red line). However, the condition with 10 mM NH_4Cl at pH 6.5 (green line) was not able to induce significant upshift of the S_2 state carboxylate mode at ∼1365 cm^{-1}. Our results showed a clear difference between pH 6.5 and 7.5 on the concentration dependence of the NH_4Cl-induced spectral changes in the $S_2Q_A^-/S_1Q_A$ spectra of PSII.

Figure 7 shows the low-frequency (630−510 cm^{-1}) $S_2Q_A^-/S_1Q_A$ FTIR difference spectra of hydrated HTG PSII RCC samples at pH 7.5 with 100 mM NaCl (blue line), 100 mM

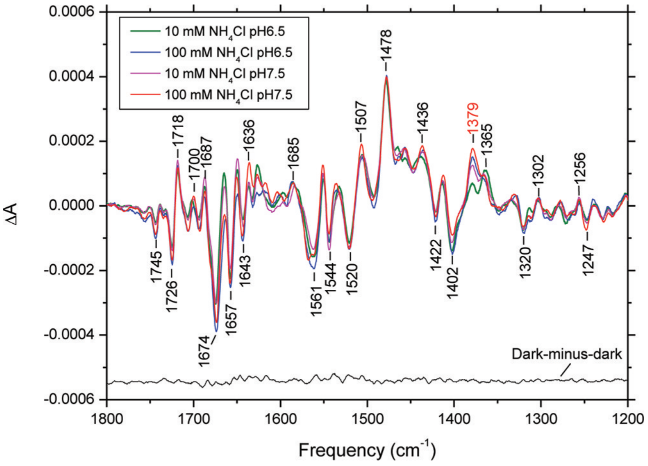

Figure 6. Mid-frequency $S_2Q_A^-/S_1Q_A$ FTIR difference spectra of hydrated PSII samples with 10 mM NH_4Cl at pH 6.5 (green line), 100 mM NH_4Cl at pH 6.5 (blue line), 10 mM NH_4Cl at pH 7.5 (magenta line), and 100 mM NH_4Cl at pH 7.5 (red line). The sample suspension included 0.1 mM DCMU. The FTIR measurement was performed at 250 K. Spectra obtained with 6−7 samples were averaged. The intensity of each spectrum has been normalized with respect to the Q_A^- band at 1478 cm^{-1}.

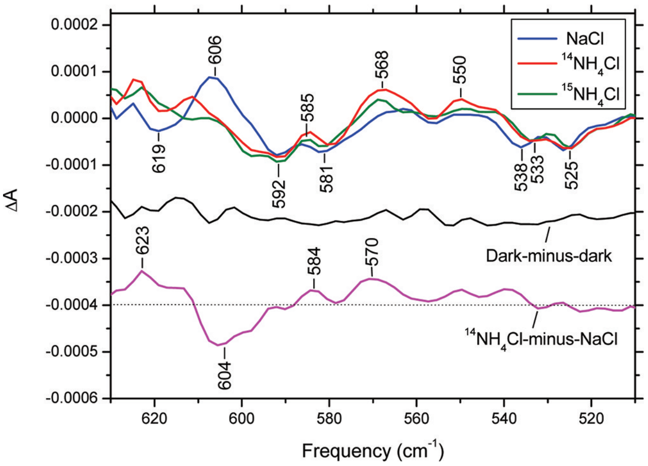

Figure 7. Low-frequency $S_2Q_A^-/S_1Q_A$ FTIR difference spectra of hydrated PSII samples with 100 mM NaCl (blue line), 100 mM $^{14}NH_4Cl$ (red line), or 100 mM $^{15}NH_4Cl$ (green line). The double-difference $^{14}NH_4Cl$-minus-NaCl spectrum (magenta line) shown at the bottom was obtained by subtracting the $S_2Q_A^-/S_1Q_A$ FTIR difference spectrum of PSII samples with 100 mM NaCl (blue line) from the $S_2Q_A^-/S_1Q_A$ FTIR difference spectrum of PSII samples with 100 mM $^{14}NH_4Cl$ (red line). The sample suspension included 0.1 mM DCMU. The FTIR measurement was performed at 250 K. Spectra obtained with 30−40 samples were averaged.

$^{14}NH_4Cl$ (red line), or 100 mM $^{15}NH_4Cl$ (green line). A positive band at 606 cm^{-1} in the $S_2Q_A^-/S_1Q_A$ FTIR difference spectrum of the NaCl control samples was apparently diminished in the samples treated with NH_4Cl. More detailed spectral changes, a negative band at 604 cm^{-1} and positive bands at ~623, ~584, and ~570 cm^{-1}, were observed in the double-difference $^{14}NH_4Cl$-minus-NaCl and $S_2Q_A^-/S_1Q_A$ FTIR spectra of PSII (magenta line). This 606 cm^{-1} mode in the $S_2Q_A^-/S_1Q_A$ FTIR difference spectrum of the NaCl control samples was either diminished or underwent a large frequency shift, e.g., shifted to the 623 cm^{-1} region or to another spectral region in the NH_4Cl-treated PSII samples. In previous studies, the 606 cm^{-1} mode was assigned to the Mn−O−Mn cluster vibrational mode of the S_2 state OEC.[27−29] In contrast, there is no apparent ^{15}N-induced frequency shift in the double-difference $^{15}NH_4Cl$-minus-$^{14}NH_4Cl$ and $S_2Q_A^-/S_1Q_A$ FTIR spectrum of PSII (data not shown). We speculate that NH_3-derived vibrational modes may be too weak (or too broad) to be detected in the spectral region (630−510 cm^{-1}) under our current experimental conditions or that they may appear in a different spectral region. Our low-frequency FTIR results clearly demonstrated that NH_4Cl induced a significant alteration on the core structure of the Mn_4CaO_5 cluster in PSII.

■ DISCUSSION

Because of the structural similarity between NH_3 and H_2O and ability of NH_3 to inhibit photosynthetic water oxidation, the NH_3 binding site on the OEC might occur at the substrate water binding site.[3−9] In the crystal structure of the Mn_4CaO_5 cluster in PSII at 1.9 Å resolution, four water molecules were associated with the Mn_4CaO_5 cluster.[1] Two of them are associated with one Mn atom, and the other two are associated with the Ca atom. The four coordinated water molecules on the OEC are involved in a hydrogen-bonded network linking the Mn_4CaO_5 cluster and Y_Z.[25] The bond distances between oxygen atoms of coordinated water molecules and their neighboring water molecules range from 2.8 to 3.3 Å.[25] The bond distances indicate that most of the O−H groups of the coordinated water molecules on the Mn_4CaO_5 cluster are likely weakly hydrogen bonded and may appear in the weakly hydrogen-bonded (3750−3500 cm^{-1}) region of the FTIR spectra. In addition, substrate water exchange experiments showed at least one of the substrate water molecules already bound in the S_1 state.[23,24] Noguchi and colleagues reported flash-induced difference spectra of S-state transitions in the weakly H-bonded OH-stretching region.[15−18] The water (or hydroxide) molecules detected in FTIR difference spectra are potential candidates for substrate water molecules in PSII water oxidation reactions. One active water molecule on the OEC which gave rise to the S_1 band at ~3585 cm^{-1} and the S_2 band at ~3618 cm^{-1} was identified in the light-induced S_2/S_1 FTIR difference spectrum of the OEC in PSII core complexes at pH 6.5 from *Thermosynechococus elongatus* at 250 K[16] and during the S state cycle at 10 °C.[18] The previous FTIR study used decoupling experiments with H_2O/D_2O to show the considerably asymmetric structure of this active water molecule.[16] One of the OH groups in this active molecule is weakly H-bonded, and the other is strongly so.[16]

Previous EPR studies on NH_3-treated PSII samples demonstrated that alterations of the S_2 state multiline EPR signal occur when samples that have been illuminated at 200 K are subsequently "annealed" above 250 K.[7,8] These results suggest that NH_3 binds directly to the Mn site after the S_2 state forms.[7,8] If NH_3 displaces one of the coordinated water molecules on the OEC, we may see the disappearance of OH stretching mode(s) of this coordinated water molecule in the weakly hydrogen-bonded (3750−3500 cm^{-1}) region of the S_2/S_1 FTIR difference spectrum of NH_3-treated PSII samples. The positive band at ~3612 cm^{-1} and the negative band at ~3584 cm^{-1} in the $S_2Q_A^-/S_1Q_A$ spectrum of spinach PSII samples at pH 7.5 (Figure 1) correspond to bands at ~3618 and ~3585 cm^{-1} in the S_2/S_1 difference spectrum of *Thermosynechococcus elongatus* PSII core complexes at pH 6.5.[16] Our results clearly showed that NH_3 did not replace this active water molecule on (or near) the OEC at pH 7.5 during the S_1 to S_2 transition at 250 K. However, we observed that NH_4Cl induced small frequency shifts (about 2−3 cm^{-1}) of these two water modes in the $S_2Q_A^-/S_1Q_A$ spectra of NH_3-treated PSII samples. Our results suggest that NH_4Cl induced a small but significant structural perturbation on this active water molecule on (or near) the OEC. Furthermore, our results do not rule out the possibility that NH_3 may replace one of the coordinated water molecules on the OEC which have strong hydrogen-bonding in both the OH groups. These bands would occur in the strongly hydrogen-bonded OH region and would have been difficult to detect in this study.

The other possibility is that NH_3 may replace one of the bridging oxygen atoms in the Mn_4CaO_5 cluster during the S_1 to S_2 transition at 250 K. Previous EPR, ESEEM, and EXAFS studies provided evidence that NH_3 might form an imido (NH) or amido (NH_2) bridge between Mn ions in place of a μ-oxo bridge.[4,9,10] In addition, in the structure of the Mn_4CaO_5 cluster in PSII at 1.9 Å resolution, the apparently longer distances between the O5-bridging oxygen atom and neighboring metal atoms suggested that the corresponding bonds are weak.[1] O5 was proposed to exist as a hydroxide ion in the S_1 state and may provide one of the substrates for O−O bond formation.[1] Previous low-frequency FTIR studies showed that a S_2 Mn−O−Mn cluster vibrational mode at 606 cm^{-1} in the S_2/S_1 spectrum was clearly downshifted to 596 cm^{-1} by ^{18}O water exchange.[27−29] These results indicate that one of the bridged oxygen atoms in this Mn−O−Mn cluster is exchangeable and accessible by water.[27] We speculate that this bridged oxygen atom may correspond to the O5-bridging oxygen atom in the Mn_4CaO_5 cluster of PSII.[1,25] Our results in Figure 7 show that the Mn−O−Mn cluster vibrational mode at ∼606 cm^{-1} was diminished or underwent a large shift in the $S_2Q_A^-/S_1Q_A$ spectrum of NH_3-treated PSII samples. Our results suggested that NH_3 induced a significant alteration on the core structure of the Mn_4CaO_5 cluster in PSII. Similar effects were observed in previous low-frequency FTIR studies on the PSII samples when Ca^{2+} was replaced with Sr^{2+} [27] or when replacing direct ligands to the Mn_4CaO_5 cluster, such as D1-glutamate 189 with glutamine[30] or D1-asparate 170 with histidine.[31] Therefore, our FTIR results support the proposal that NH_3 binds directly to the Mn site on the OEC during the S_1 to S_2 transition.[7,8] Future FTIR experiments to identify vibrational modes of the imido (NH) or amido (NH_2) bridge of the Mn cluster in the low-frequency region (1000−350 cm^{-1}) of the S_2/S_1 spectrum of NH_3-treated PSII samples are required to determine whether NH_3 may replace one of the bridging oxygen atoms in the Mn_4CaO_5 cluster during the S_1 to S_2 transition at 250 K.[4,9,10]

A previous study identified the FTIR bands of internal water molecules around the quinone binding site in the bacterial reaction center of *Rhodobacter sphaeroides*.[32] In the weakly hydrogen-bonded OH stretching region of their Q_A^-/Q_A spectra, one band appeared at 3664 cm^{-1} in the formation of Q_A, and three bands disappeared at 3657, 3622, and 3587 cm^{-1}.[32] The results demonstrated that several weakly hydrogen-bonded water molecules were perturbed by Q_A reduction in the bacterial reaction center.[32] The authors proposed that the reorientation of these weakly hydrogen-bonded water molecules may play an important role in stabilizing the charge-separated state of the quinone molecules in bacterial reaction centers.[32] In this study, we detected a positive band at 3658 cm^{-1} in the Q_A^-/Q_A spectra which is sensitive to D_2O and ^{18}O water exchanges. Our result provides evidence that one weakly hydrogen-bonded water molecule undergoes structural changes in the formation of Q_A^- in PSII and may play a significant role in stabilizing its charge-separated state.

A recent FTIR study identified an inhibitory effect of the ammonium cation on the PSII/OEC.[14] The NH_4Cl treatment at pH 6.5 and 5.5 induced significant changes in the COO^- stretching regions in the light-induced S_2/S_1 FTIR difference spectra of PsbP- and PsbQ-depleted PSII samples at 283 K.[14] The authors of this study proposed that the ammonium cation interacts with carboxylate groups coupled to the Mn cluster as direct ligands or proton transfer mediators and inhibits the oxygen evolution reaction.[14] Their FTIR experimental conditions (pH 6.5 and 5.5 and 283 K) and the proposed inhibition mechanism of ammonium cation on the OEC are different from the conditions (pH 7.5 and 250 K) and the proposed mechanism present here. This FTIR study also reported that 100 mM NH_4Cl induced a large upshift of the S_2 state carboxylate mode at 1365 cm^{-1} in the $S_2Q_A^-/S_1Q_A$ spectrum of PsbP- and PsbQ-depleted PSII membranes at 250 K and pH 6.5 but did not induce significant alteration of the multiline EPR signals under the same condition.[14] They raised the question that the upshift of this S_2 state carboxylate mode at 250 K may arise from NH_4^+ and not from NH_3. However, our FTIR results in Figure 6 show a clear difference between pH 6.5 and 7.5 on the NH_4Cl concentration dependence of the upshift of the S_2 state carboxylate mode at 1365 cm^{-1} in the $S_2Q_A^-/S_1Q_A$ spectra of PSII. Our results provide evidence that the upshift of the 1365 cm^{-1} mode in PSII samples containing 100 mM NH_4Cl at pH 6.5 and 250 K is primarily due to the effect of NH_3 molecules. Our previous FTIR results also showed strong correlations between the conditions (dependences on excitation temperature and NH_3 concentration and the steric requirement for the amine effects) that give rise to the NH_3-induced upshift of the 1365 cm^{-1} mode and those that give rise to the modified S_2 state multiline EPR signal.[11] Taken together, our FTIR results strongly suggest that NH_3 induced the upshift of the 1365 cm^{-1} mode in the $S_2Q_A^-/S_1Q_A$ spectra of NH_4Cl-treated PSII samples at 250 K.

AUTHOR INFORMATION

Corresponding Author

*Phone: 886-2-27871169. Fax: 886-2-27827954. E-mail: chuha@gate.sinica.edu.tw.

Funding

This work was supported by the National Science Council in Taiwan (NSC 99-2627-M-001−004) and by Academia Sinica to H.A.C.

ACKNOWLEDGMENTS

We thank the reviewers for helpful comments on the manuscript.

ABBREVIATIONS

DCMU, 3-(3,4-dichloro-phenyl)-1,1-dimethylurea; EPR, electron paramagnetic resonance; ESEEM, electron spin echo envelope modulation; EXAFS, extended X-ray absorption fine structure; FTIR, Fourier transform infrared; HEPES, *N*-(2-hydroxyethyl)piperazine-*N*′-2-ethanesulfonic acid; HTG, *n*-heptyl-β-D-thioglucoside; Mes, 2-(*N*-morpholino)-ethanesulfonic acid; OEC, oxygen-evolving complex; OTG, octyl-β-D-thioglucopyranoside; PSII, photosystem II; Q_A, the primary quinone electron acceptor in PSII.

REFERENCES

(1) Umena, Y., Kawakami, K., Shen, J.-R., and Kamiya, N. (2011) Crystal structure of oxygen-evolving photosystem II at a resolution of 1.9 Å. *Nature 473*, 55−60.

(2) Kern, J., and Renger, G. (2007) Photosystem II: structure and mechanism of the water:plastoquinone oxidoreductase. *Photosynth. Res. 94*, 183−202.

(3) Debus, R. J. (1992) The manganese and calcium ions of photosynthetic oxygen evolution. *Biochim. Biophys. Acta 1102*, 269−352.

(4) Brudvig, G. W., and Beck, W. F. (1992) Oxidation-reduction and ligand-substitution reactions of the oxygen-evolving center of photosystem II, in *Manganese Redox Enzymes* (Pecoraro, V. L., Ed.) pp 119−141, VCH Publishers, New York.

(5) Sandusky, P. O., and Yocum, C. F. (1984) The chloride requirement for photosynthetic oxygen-evolution: Analysis of the effects of chloride and other anions on amine inhibition of the oxygen-evolving complex. *Biochim. Biophys. Acta 766*, 603−611.

(6) Sandusky, P. O., and Yocum, C. F. (1986) The chloride requirement for photosynthetic oxygen-evolution: factors affecting nucleophilic displacement of chloride from the oxygen-evolving complex. *Biochim. Biophys. Acta 849*, 85−93.

(7) Beck, W. F., de Paula, J. C., and Brudvig, G. W. (1986) Ammonia binds to the manganese site of the O_2-evolving complex of photosystem II in the S_2 state. *J. Am. Chem. Soc. 108*, 4018−4022.

(8) Beck, W. F., and Brudvig, G. W. (1986) Binding of amines to the O_2-evolving center of photosystem II. *Biochemistry 25*, 6479−6486.

(9) Britt, R. D., Zimmermann, J.-L., Sauer, K., and Klein, M. P. (1989) Ammonia binds to the catalytic Mn of the oxygen-evolving complex of photosystem II: evidence by electron spin−echo envelope modulation spectroscopy. *J. Am. Chem. Soc. 111*, 3522−3532.

(10) Dau, H., Andrews, J. C., Roelofs, T. A., Latimer, M. J., Liang, W., Yachandra, V. K., Sauer, K., and Klein, M. P. (1995) Structural consequences of ammonia binding to the manganese center of the photosynthetic oxygen-evolving complex: An X-ray absorption spectroscopy study of isotropic and oriented photosystem II particles. *Biochemistry 34*, 5274−5287.

(11) Chu, H. A., Feng, Y. W., Wang, C. M., Chiang, K. A., and Ke, S. C. (2004) Ammonia-induced structural changes of the oxygen-evolving complex in photosystem II as revealed by light-induced FTIR difference spectroscopy. *Biochemistry 43*, 10877−10885.

(12) Fang, C. H., Chiang, K. A., Hung, C. H., Chang, K., Ke, S. C., and Chu, H.-A. (2005) Effects of ethylene glycol and methanol on ammonia-induced structural changes of the oxygen-evolving complex in photosystem II. *Biochemistry 44*, 9758−9765.

(13) Noguchi, T., Ono, T., and Inoue, Y. (1995) Direct detection of a carboxylate bridge between Mn and Ca^{2+} in the photosynthetic oxygen-evolving center by means of Fourier transformed infrared spectroscopy. *Biochim. Biophys. Acta 1228*, 189−200.

(14) Tsuno, M., Suzuki, H., Kondo, T., Mino, H., and Noguchi, T. (2011) Interaction and inhibitory effect of ammonium cation in the oxygen evolving center of photosystem II. *Biochemistry 50*, 2506−2514.

(15) Noguchi, T. (2008) FTIR detection of water reactions in the oxygen-evolving centre of photosystem II. *Philos. Trans. R. Soc. London, B 363*, 1189−1195.

(16) Noguchi, T., and Sugiura, M. (2000) Structure of an active water molecule in the water oxidizing complex of photosystem II as studies by FTIR spectroscopy. *Biochemistry 39*, 10943−10949.

(17) Noguchi, T., and Sugiura, M. (2002) Flash-induced FTIR difference spectra of the water oxidizing complex in moderately hydrated photosystem II core films: effect of hydration extent on S-state transitions. *Biochemistry 41*, 2322−2330.

(18) Noguchi, T., and Sugiura, M. (2002) FTIR detection of water reactions during the flash-induced S-state cycle of the photosynthetic water oxidizing complex. *Biochemistry 41*, 15706−15712.

(19) Mishra, R. K., and Ghanotakis, D. F. (1994) Selective extraction of CP 26 and CP 29 proteins without affecting the binding of the extrinsic proteins (33, 23 and 17 kDa) and the DCMU sensitivity of a Photosystem II core complex. *Photosyn. Res. 42*, 37−42.

(20) Hasegawa, K., Kimura, Y., and Ono, T. (2004) Oxidation of the Mn cluster induces structural changes of NO_3^- functionally bound to the Cl^- site in the oxygen-evolving complex of photosystem II. *Biophys. J. 86*, 1042−1050.

(21) Schmidt, K. H., and Muller, A. (1976) Vibrational spectra and force constants of pure amine complexes. *Coord. Chem. Rev. 19*, 41−97.

(22) Noguchi, T., and Sugiura, M. (2003) Analysis of flash-induced FTIR difference spectra of the S-state cycle in the photosynthetic water oxidizing complex by uniform ^{15}N and ^{13}C isotope labeling. *Biochemistry 42*, 6035−6042.

(23) Hillier, W., and Wydrzynski, T. (2000) The affinities for the two substrate water binding sites in the O_2 evolving complex of photosystem II vary independently during S-state turnover. *Biochemistry 39*, 4399−4405.

(24) Hendry, G., and Wydrzynski, T. (2002) The two substrate-water are already bound to the oxygen-evolving complex in the S2 state of photosystem II. *Biochemistry 41*, 13328−13334.

(25) Kawakami, K., Umena, Y., Kamiya, N., and Shen, J.-R. (2011) Structure of the catalytic, inorganic core of the oxygen-evolving photosystem II at 1.9 Å resolution. *J. Photochem. Photobiol. B 104*, 9−18.

(26) Eisenburg, D., and Kauzmann, W. (1969) *The Structure and Properties of Water*, Oxford Press, London.

(27) Chu, H.-A., Sackett, H., and Babcock, G. T. (2000) Identification of a Mn-O-Mn cluster vibrational mode of the oxygen-evolving complex in photosystem II by low-frequency FTIR spectroscopy. *Biochemistry 39*, 14371−14376.

(28) Chu, H.-A., Hillier, W., Law, N. A., and Babcock, G. T. (2001) Vibrational spectroscopy of the oxygen-evolving complex and of manganese model compounds. *Biochim. Biophys. Acta 1503*, 69−82.

(29) Kimura, Y., Ishii, A., Yamanari, T., and Ono, T. (2005) Water-sensitive low-frequency vibrations of reaction intermediates during S-state cycling in photosynthetic water oxidation. *Biochemistry 44*, 7613−7622.

(30) Kimura, Y., Mizusawa, N., Ishii, A., Nakazawa, S., and Ono, T. (2005) Changes in structural and functional properties of oxygen-evolving complex induced by replacement of D1-glutamate 189 with glutamine in photosystem II. *J. Biol. Chem. 280*, 37895−37900.

(31) Chu, H.-A., Debus, R. J., and Babcock, G. T. (2001) D1-Asp 170 is structurally coupled to the oxygen evolving complex in photosystem II as revealed by light-induced Fourier transform infrared difference spectroscopy. *Biochemistry 40*, 2312−2316.

(32) Iwata, T., Paddock, M. L., Okamura, M. Y., and Kandori, H. (2009) Identification of FTIR bands due to internal water molecules around the quinone binding site in the reaction center from *Rhodobacter sphaeroides*. *Biochemistry 48*, 1220−1229.